



Zou, Huiming and Wang, Wei and Zhang, Guiying and Qin, Fei and Tian, Changqing and Yan, Yuying (2016) Experimental investigation on an integrated thermal management system with heat pipe heat exchanger for electric vehicle. *Energy Conversion and Management*, 118 . pp. 88-95. ISSN 0196-8904

Access from the University of Nottingham repository:

<http://eprints.nottingham.ac.uk/41059/1/Experimental%20investigation%20on%20an%20integrated%20system-revised2%20%28HZou%20and%20YYan%29.pdf>

Copyright and reuse:

The Nottingham ePrints service makes this work by researchers of the University of Nottingham available open access under the following conditions.

This article is made available under the Creative Commons Attribution Non-commercial No Derivatives licence and may be reused according to the conditions of the licence. For more details see: <http://creativecommons.org/licenses/by-nc-nd/2.5/>

A note on versions:

The version presented here may differ from the published version or from the version of record. If you wish to cite this item you are advised to consult the publisher's version. Please see the repository url above for details on accessing the published version and note that access may require a subscription.

For more information, please contact eprints@nottingham.ac.uk

**Experimental investigation on an integrated thermal management system
with heat pipe heat exchanger for electric vehicle**

Huiming Zou^a, Wei Wang^c, Guiying Zhang^{a,b}, Fei Qin^{a,b}, Changqing Tian^a,
Yuying Yan^d

a.Beijing Key Laboratory of Thermal Science and Technology and Key Laboratory of Cryogenics,
Technical Institute of Physics and Chemistry, CAS, Beijing 100190, P. R. China,
zouhuiming@mail.ipc.ac.cn

b.University of Chinese Academy of Sciences, Beijing, China

c.China FAQ Group Corporation R&D Center, Changchun, China

d.HVACR & Heat Transfer Research Group, Faculty of Engineering, University of Nottingham,
U.K.

Abstract:

An integrated thermal management system combining a heat pipe battery cooling/preheating system with the heat pump air conditioning system is presented to fulfill the comprehensive energy utilization for electric vehicles. A test bench with battery heat pipe heat exchanger (HPHE) and heat pump air conditioning for a regular five-chair electric car is set up to research the performance of this integrated system under different working conditions. The investigation results show that as the system is designed to meet the basic cabinet cooling demand, the additional parallel branch of battery chiller is a good way to solve the battery group cooling problem, which can supply about 20% additional cooling capacity without input power increase. Its coefficient of performance(COP) for cabinet heating is around 1.34 at -20°C out-car temperature and 20°C in-car temperature. The specific heat of the battery group is tested about 1.24 kJ/kg·°C. There exists a necessary temperature condition for the HPHE to start action. The heat pipe heat transfer performance is around 0.87 W/°C

27 on cooling mode and $1.11 \text{ W/}^{\circ}\text{C}$ on preheating mode. The gravity role makes the heat
28 transfer performance of the heat pipe on preheating mode better than that on cooling
29 mode.

30

31 **Key words:** Electric vehicles, Heat pump, Heat pipe, Battery temperature control,
32 Thermal management

33 **Nomenclature:**

34 A_{hp} contact superficial area with coolant of each heat pipe (m^2)

35 c_b specific heat of battery group ($\text{kJ/kg}^{\circ}\text{C}$)

36 c_c specific heat of coolant ($\text{kJ/kg}^{\circ}\text{C}$)

37 m_b mass of battery group (kg)

38 m_c mass of coolant (kg)

39 n heat pipe number

40 Q_{bi} batteries internal heat variation (kW)

41 Q_c cooling capacity by battery chiller (kW)

42 Q_{ci} coolant internal heat variation (kW)

43 Q_g generated heat by batteries (kW)

44 Q_p preheating heat by PTC (kW)

45 Q_t transferred heat by HPHE (kW)

46 q_{hp} heat transfer coefficient of each heat pipe ($\text{W/}^{\circ}\text{C}$)

47 T_{ba} average temperature of battery group ($^{\circ}\text{C}$)

| | | |
|----|------------|-------------------------------------------------------------------------------------------------|
| 48 | T_{bo} | coolant outlet temperature ($^{\circ}\text{C}$) |
| 49 | T_{bi} | coolant inlet temperature ($^{\circ}\text{C}$) |
| 50 | T_{ca} | coolant average temperature ($^{\circ}\text{C}$) |
| 51 | ΔT | average temperature difference between the battery group and the coolant ($^{\circ}\text{C}$) |
| 52 | t | time (s) |

53 **1. Introduction**

54 Electric vehicle (EV) is an important development orientation to alleviate the
55 traditional automobile exhaust problem. However, thermal management including
56 battery temperature control and cabinet air conditioning is a big challenge for EV, as
57 the traditional engine and oil tank are replaced by electric motor and battery groups.

58 Lots of heat inside of the battery generated by the electrochemical reaction will
59 raise the battery temperature up sharply, affect its working efficiency badly and even
60 cause safety problem [1, 2]. Sato[3] analyzed the thermal behavior of lithium-ion
61 batteries showing that when the battery temperature was over 50°C , charging
62 efficiency and life cycle would be considerably diminished. Khateeb et al. [4] pointed
63 out that the safety of the Li-ion battery would descend when it operated at the
64 temperature range of $70\text{-}100^{\circ}\text{C}$. Studies have shown that there is a necessary
65 temperature range for battery to make sure its performance and service life. Pesaran [5]
66 presented that the best range of operating temperature for batteries such as lead-acid,
67 NiMH, and Li-ion are from 25 to 40°C and suitable temperature distribution from
68 module to module is below 50°C . To control the batteries in the suitable temperature

range, there are several methods presented [6-12], such as by air directly, by liquid with plate heat exchanger or by refrigerant phase change with plate or pipe heat exchanger. However, investigations on the thermal behavior of batteries [5,13-14] show that the relationship between the generated heat and discharge rate is nonlinear direct ratio and the higher the discharge rate is, the quicker the increase rate of the generated heat will be. While the discharge rate changes with the working conditions such as acceleration, deceleration, uphill, and downhill. So generated heat of the battery is variable and its instantaneous value is very high. This means the cooling capacity of the battery temperature control system with these normal methods has to be set high enough to avoid the battery on extremely high temperature and lead to an over-size thermal management system. Therefore it is very significant to search for a more efficient battery heat-transfer method to simplify the EV thermal management system.

Heat pipe, as a high efficient heat-transfer device combining the principles of both thermal conductivity and phase transition, is a novel idea to apply on the temperature control of EV battery [15]. Actually, because of its highly effective thermal conductivity, heat pipe has been applied successfully in many fields such as electron cooling, solar heater and energy recovering [16, 17]. As for the above mentioned EV battery thermal characteristics, heat pipes between the batteries can help transfer the heat out to the coolant so that the batteries can be maintained in the best operating temperature range under variable working conditions and the

temperature difference between batteries can be eliminated [18]. Moreover, because the coolant system has enough thermal capacity, the cooling load can be much lower than that of the instant cooling method. It just needs to meet the average heat dissipation demand instead of the peak generated heat during high discharge rate conditions. Therefore, heat pipe is a promising development orientation for batteries thermal management of EV. Authors' initial investigations have shown that the heat pipe cooling is an effective method [19]. However, the previous study results were mainly concentrating on the basic thermal performance of a single heat pipe unit with a simple experimental apparatus. The thermal performance of the heat pipe heat exchanger (HPHE) for the practical EV battery group still has not been researched, which might be different from that of the single heat pipe because of cluster effect.

On the other hand, since EV has no engine to drive compressor for cooling and no waste engine heat for heating, heat pump system with motor-driven compressor is an important development trend. The investigation on the performance of heat pump system has become a major topic of EV air-conditioning. Suzuki and Katsuya [20] proposed a heat pump system for electric vehicle with functions of cooling, heating, demisting and dehumidifying and their experimental results showed the feasibility of heat pump. However, heat pump system has a shortcoming that its heating capacity drops sharply with the decreasing outdoor temperature. Hosoz and Direk [21, 22] indicated this feature by investigating the performance of R134a heat pump system transformed for the original automobile air conditioning system. In recent years many

advances on heat pump system for EV have been presented [23]. Authors [24, 25] have also engaged in the heat pump performance improvement with injection technology and got notable achievement in system heating capacity and COP under extremely cold condition. However when it comes to practical performance of the heat pump system combining with battery temperature control system, there is few literature either.

In this paper, an integrated thermal management system combining a HPHE for battery cooling/preheating with a heat pump air conditioning is presented to investigate its performance characteristics on different working conditions. Cooling and heating performances of the system, as well as the thermal performance of HPHE, are investigated by bench test, hoping to present a significative reference for the EV thermal management.

2. System description and experimental bench setup

2.1 System description

Fig.1 shows the diagram of the heat pump coupling with battery cooling /preheating system based on regular five-chair electric cars and takes R134a as refrigerant. Its working temperature ranges from -20°C to 45°C. The heat pump system mainly consists of a variable-frequency scroll compressor, an outside heat exchanger with a fan, a liquid vapour separator, four refrigerant valves (RV), a condenser followed by an expansion valve (EXV1) for cabinet heating, an refrigerant-air

evaporator following with EXV2 for cabinet cooling and a refrigerant-water
 evaporator for battery cooling called battery chiller. The refrigerant-air evaporator and
 condenser are installed in the ventilation duct. The system is switched by the RVs for
 cooling or heating. The battery cooling/preheating system also applies a water-air heat
 exchanger in front of the car to utilize the natural cooling source and a Positive
 Temperature Coefficient (PTC) heater to preheat the battery in cold season. A HPHE
 is installed among the battery group, called battery heat exchanger box here. Please
 refer the reference [20] for more details of the HPHE.

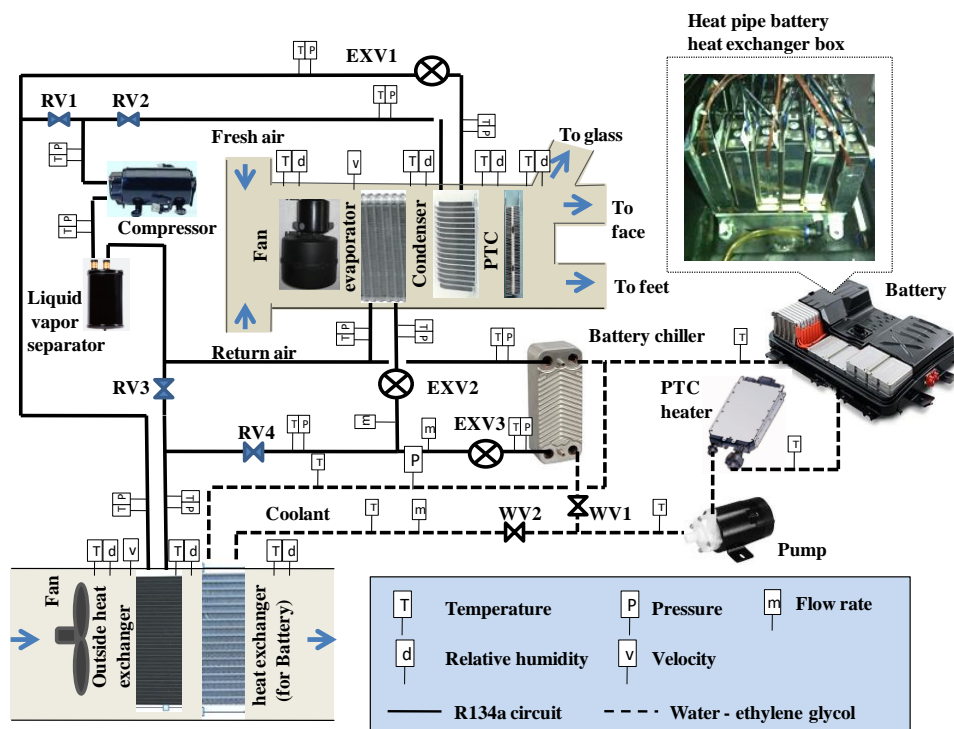


Fig.1. Diagram of the heat pump coupling with the battery cooling/preheating system

2.2 Experimental bench

Correspondingly a test bench is set up inside of a psychrometer testing room to
 investigate the performance of this system. The experiments are carried out on

cooling and heating mode respectively under different working conditions. On cooling mode, the refrigerant valve RV1 and RV4 are open while RV2 and RV3 are closed. The opening of expansion valves EXV2 and EXV3 are changed repeatedly to get the optimum branch refrigerant flow rate of the cabin evaporator and battery chiller. On heating mode, the refrigerant valve RV1 and RV4 are closed while RV2 and RV3 are open. The battery is preheated by the PTC heater. The coolant pipe system and battery heat exchanger box are isolated to prevent unmeasured heat loss. There are 30 real battery modules in the bench for electric cars, but the generated heat during discharging process is simulated by electric films for the sake of safety. The electric films are pasted on the two wide sides of each battery module and thermocouples are pasted on the other two narrow sides to measure the temperature response of the batteries. Each side has three thermocouples. The measurement devices of the bench are shown in Fig.1 and their parameters are shown in Table 1. The relative parameters of the bench are shown in Table 2.

Table 1 Measurement devices

| Parameter | Type | Range | Error |
|------------------------|--------------|-------------|---------------------------|
| Temperature | Thermocouple | -30 to 220℃ | $\pm 0.5^{\circ}\text{C}$ |
| Pressure | Diaphragm | 0 to 30bar | $\pm 0.5\%$ |
| Air speed | Hot bulb | 0 to 40m/s | $\pm 3\%$ |
| Mass flow rate of Ref. | Coriolis | <370kg/h | $\pm 0.1\%$ |

Table 2 Parameter of the bench

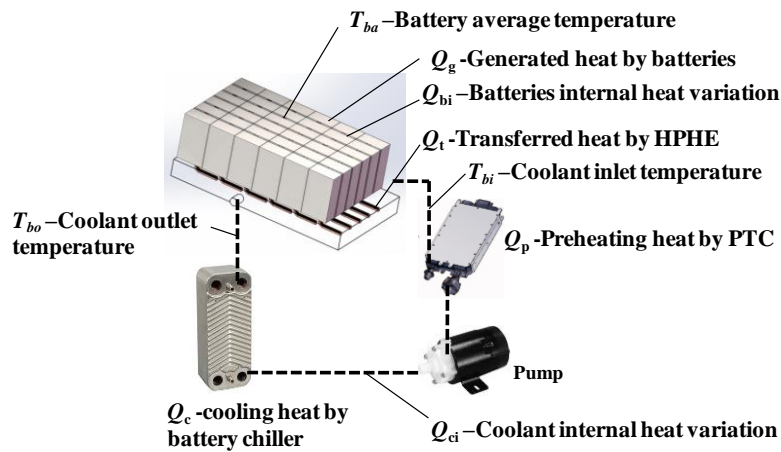
| Item | Symbol | Value(unit) |
|------|--------|-------------|
|------|--------|-------------|

| | | |
|---------------------------------------------------------|----------|------------------------|
| Mass of battery group | m_b | 16.03 kg |
| Mass of coolant | m_c | 3.96 kg |
| | | 3.334 kJ/kg°C @ -20°C |
| Specific heat of ethylene glycol coolant | c_c | 3.518 kJ/kg°C @ 35°C |
| | | 3.552 kJ/kg°C @ 45°C |
| Contact superficial area with coolant of each heat pipe | A_{hp} | 0.00188 m ² |
| Heat pipe number | n | 25 |

161

162 2.3 Calculation methodology

163 To investigate the heat transfer performance of HPHE of battery group, the
 164 experiment is carried out to simulate different working modes. The heat composition
 165 of the battery temperature control system is shown as Fig.2. The battery internal heat
 166 variation and coolant internal heat variation can be expressed as equation (1) and (2)
 167 respectively. Here heat transfer coefficient of each heat pipe q_{hp} is applied to indicate
 168 the heat transfer performance of the HPHE, which can be expressed as equation(3).



169

170

Fig.2 Heat composition of the battery group temperature control system

171

$$Q_{bi} = c_b m_b \frac{dT_{ba}}{dt} = Q_g + Q_t \quad (1)$$

172
$$Q_{ci} = c_c m_c \frac{dT_{ca}}{dt} = Q_t + Q_p + Q_c \quad (2)$$

173
$$q_{hp} = \frac{Q_t}{n\Delta T} \quad (3)$$

174 Because the system heat-transfer process goes from dynamic to steady state
175 gradually and the energy during the initial dynamic process is not balanced, it is
176 important to note that this model is only suitable for the final steady state.

177 3. Experimental result and discussion

178 3.1 Heat pump system performance

179 Table 3 shows the system cooling and heating performance under different
180 working conditions.

181 Table 3 Cooling/heating performance of the heat pump system

| Experiment No. | 1 | 2 | 3 | 4 | 5 | 6 |
|----------------------------------------------|--------|-------|--------|-------|--------|--------|
| Out-car temperature (°C) | 35 | 35 | 45 | 45 | -20 | -20 |
| In-car temperature (°C) | 27 | 27 | 45 | 45 | -20 | 20 |
| EXV1 opening (%) | 0 | 0 | 0 | 0 | 100 | 100 |
| EXV2 opening (%) | 84 | 84 | 63 | 63 | 0 | 0 |
| EXV3 opening (%) | 0 | 40 | 0 | 90 | 0 | 0 |
| Evaporator evaporating temperature (°C) | -1.49 | -0.48 | 9.96 | 11.7 | -23.13 | -21.58 |
| Super-heating temperature (°C) | 0.93 | 0.76 | 1.28 | 2.59 | 0.01 | 1.37 |
| Battery chiller evaporating temperature (°C) | -- | -4.30 | -- | 7.49 | -- | -- |
| Super-heating temperature (°C) | -- | 18.35 | -- | 0.36 | -- | -- |
| Condensing temperature (°C) | 41.18 | 41.58 | 55.4 | 54.31 | 20.78 | 58 |
| Sub-cooling temperature (°C) | 0.3 | 0 | 7.36 | 1.98 | 21.62 | 9.45 |
| Cabinet refrigerant flow rate (kg/h) | 135.16 | 134.0 | 192.01 | 180.4 | 43.2 | 47.56 |
| Cabinet cooling/heating capacity (kW) | 5.24 | 5.19 | 7.22 | 6.61 | 2.96 | 2.75 |
| Battery chiller refrigerant flow rate (kg/h) | -- | 25.36 | -- | 63.96 | -- | -- |

| | | | | | | |
|---------------------------------------|-------|-------|-------|------|-------|-------|
| Battery chiller cooling capacity (kW) | -- | 1.09 | -- | 2.31 | -- | -- |
| Theoretical compression power (kW) | 1.04 | 1.24 | 1.43 | 1.75 | 0.45 | 0.86 |
| Actual input power (kW) | 2.44 | 2.46 | 3.13 | 3.19 | 1.48 | 2.04 |
| Compression efficiency (%) | 42.51 | 50.34 | 45.53 | 55.0 | 30.27 | 42.05 |
| COP | 2.15 | 2.55 | 2.31 | 2.80 | 2.0 | 1.34 |

182

183 On cooling mode under out-car 35°C and in-car 27°C condition, the opening of
184 EXV1 is kept on 84% while that of EXV3 is changed from 0 to 40%. The evaporator
185 cooling capacity decreases lightly and the battery chiller cooling capacity increases
186 quickly. The total cooling capacity increases about 19.84% and the compressor input
187 power almost keeps the same, so the system COP increases about 18.60%. Under
188 out-car 45°C and in-car 45°C condition, the optimum opening of EXV2 is 63% and
189 that of EXV3 is 90%. And also the system total cooling capacity and COP under this
190 conditions are both increases. Compare to the out-car 35°C and in-car 27°C
191 condition, the cooling capacity for both cabin and battery as well as system COP are
192 much higher because of the lower compression ratio under this condition. The
193 experimental results of cooling performance show that the additional parallel branch
194 of battery chiller is a good way to solve the battery cooling problem, which can
195 supply about 20% additional cooling capacity without input power increase.

196 On heating mode under out-car -20°C and in-car -20°C condition, system
197 condensing temperature is about 20°C. As the in-car temperature increases to 20°C,
198 system condensing temperature increases to 58°C, heating capacity decreases from

2.96 kW to 2.75kW, the compressor input power increases from 1.48 kW to 2.04 kW, and the heating COP decreases from 2.0 to 1.34. The experimental results show that although the heating COP under -20°C in-car temperature is higher than that under 20°C because of the lower compression ratio, the compression efficiency of the scroll compressor is much lower. This is because the motor efficiency of scroll compressor drops rapidly under lower load conditions. The heating capacity is insufficient for the cabinet heating. Therefore PTC heater is suggested to be an auxiliary heat source under extremely cold weather.

3.2 Heat pipe heat exchanger performance

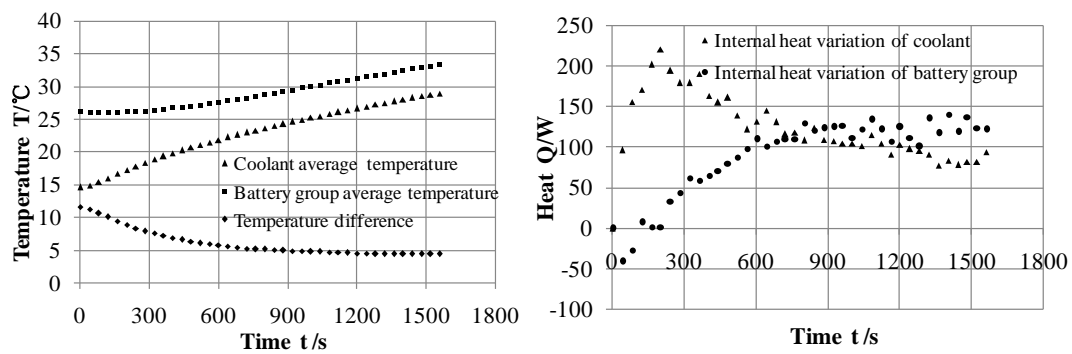
3.2.1 Testing mode without heating or cooling

Because the battery group is a composition of electrolyte, metal and heat pipe etc., and the thermal capacity characteristics of different material are different, the specific heat of battery group is uncertain. A testing experiment is carried out firstly to test the specific heat of battery group. On this mode, the coolant is circulated by the pump with neither PTC heating nor battery chiller cooling and the generated heat of battery group is dissipated to the coolant by the HPHE. The equation (1) and (2) can be transferred into equation (4).

$$c_b m_b \frac{dT_{ba}}{dt} = Q_g - c_c m_c \frac{dT_{ca}}{dt} \quad (4)$$

Fig.3(a) shows the average temperature response tendency of the battery group and the coolant from start to steady state. The temperature difference between them decreases from 11.6°C to a constant 4.4°C. Fig.3(b) shows the internal heat variation

response tendency of the battery group and the coolant. As mentioned in the above calculation methodology, the model applied for the steady state is quasi-steady and it is not suitable for the dynamic process. So the initial calculated heat shown in Fig.3(b), which goes up to more than 200W, does not present the actual heat value. The average internal heat variation of the battery group and the coolant at the steady state is around 119.4W and 83.6W respectively. Therefore according to equation (4), the specific heat of battery group can be gained, which about 1.24 kJ/kg $^{\circ}$ C. This result has also been verified by the following experiment based on the equation (1) and (2).



(a) Temperature response tendency (b) Internal heat variation response tendency

Fig.3 Experimental response tendency

Heat transfer way of the heat pipe under this condition is shown as Fig 4. The top part *a* of the heat pipe absorbs heat from battery and the fluid inside takes the heat to the bottom part *b* to dissipate to the coolant. The fluid inside of the heat pipe evaporates at the top part, goes down to the bottom part by pressure, and goes up by capillary action after condensation. The heat transfer performance of each heat pipe (Fig.5) can be obtained by equation (3) and it shows that as the experiment goes to steady state the heat transfer performance of each heat pipe gets to a relative stable value, which is around 0.86W/ $^{\circ}$ C.

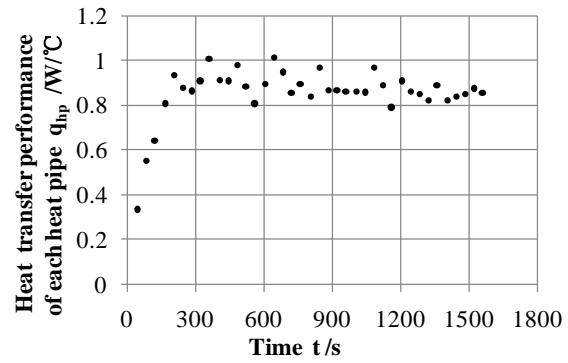
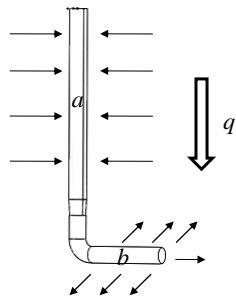


Fig.4 Heat transfer way of the heat pipe

Fig.5 Heat transfer performance of each heat pipe

3.2.2 Cooling mode

On this mode the coolant is circulated by the pump with battery chiller cooling and the battery group generates heat. The cooling capacity of the battery chiller is adjusted by changing the opening degree of EXV3.

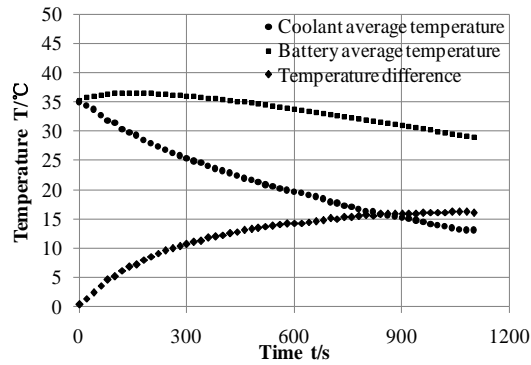
Fig.6 shows the temperature response of the battery cooling process. At the beginning, the battery group and the coolant are on the same temperature condition. As the cooling mode starts, the coolant average temperature inside of the battery exchanger box decreases quickly. While the battery average temperature increases to a higher value firstly and then begins to decrease with the coolant. It is worthy of mention that as the battery average temperature increases to the highest point, the temperature differences between the coolant and the battery group are all in the range of 7~8°C under every experimental condition. This result shows that at the beginning of this experimental mode, the battery begins to generate heat as it supplies power while the HPHE does not start until the temperature difference goes up to 7~8°C. Therefore the battery group temperature will go up before the HPHE starts to transfer heat from the battery to the coolant. And finally the battery temperature decreases to

its suitable range. The battery cooling rate depends on the EXV3 opening degree.

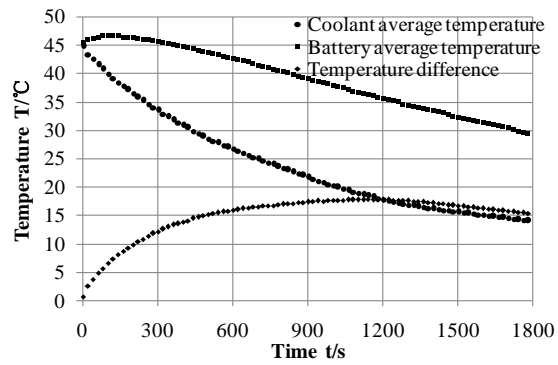
Under the conditions of 33% EXV3 opening degree, it takes about 1040s to be cooled

from 35°C to 30°C, 1720 s from 45°C to 30°C. Under the conditions of 60% EXV3

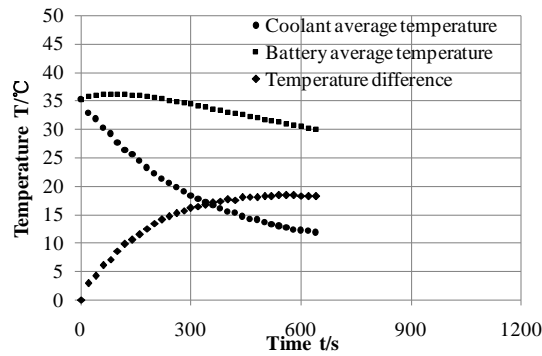
opening, it takes 600s from 35°C to 30°C, 1180s from 45°C to 30°C.



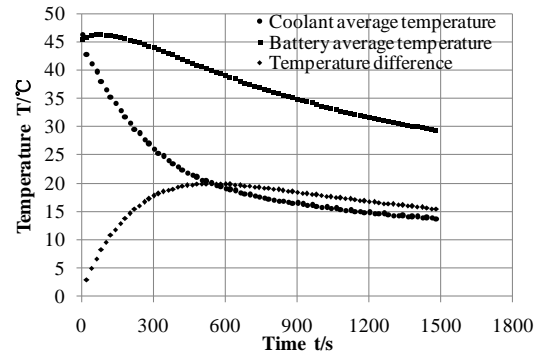
(a)35°C/33%



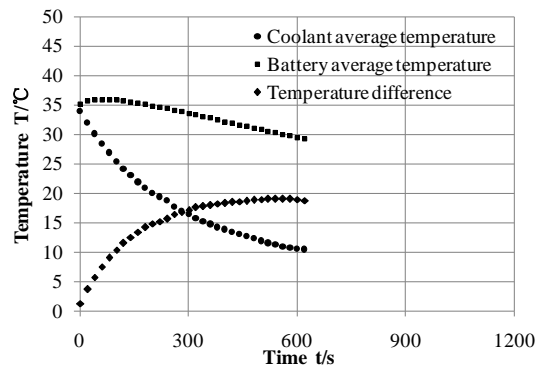
(b)45°C/33%



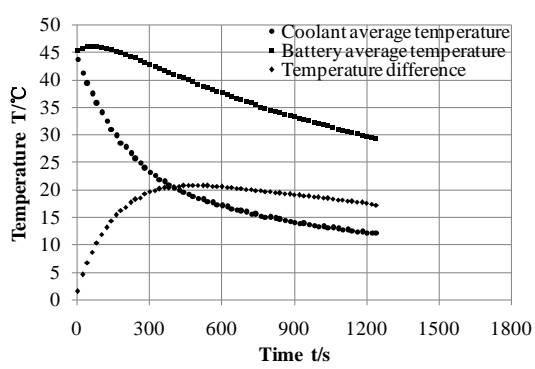
(c)35°C/60%



(d)45°C/60%



(e)35°C/100%



(f)45°C/100%

Fig.6 Temperature response tendency on cooling mode

Fig.7 shows the heat transfer performance of each heat pipe according to equations (1)~(3). Heat transfer way of the heat pipe under this condition is the same as fig 3. The results show that as the system runs to steady state the values of the heat pipe heat transfer performance on different working conditions go to be coincident, which is around $0.87 \text{ W/}^{\circ}\text{C}$. This result is also fitting very well with the above experimental result. According to this result, the total heat transfer performance of the HPHE is easily to be estimated, so that the temperature difference between coolant and battery group can be determined accordingly in the real application.

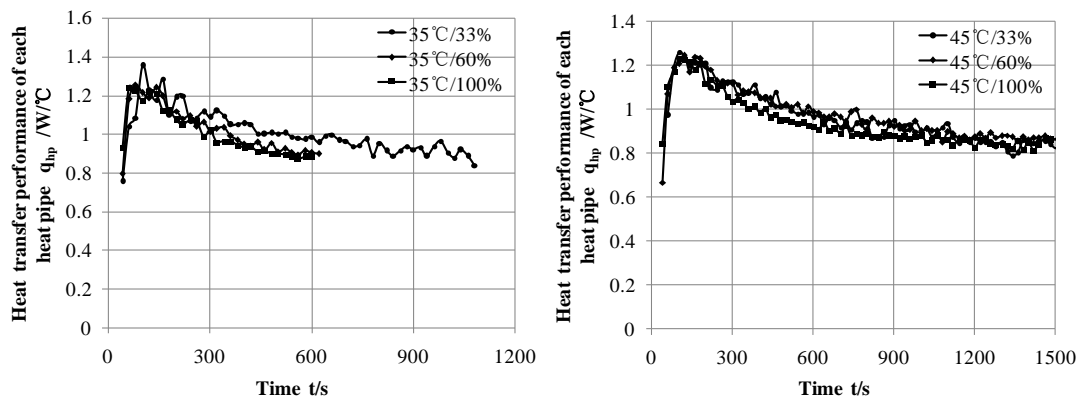


Fig.7 Heat transfer performance of each heat pipe on cooling mode

3.2.3 Preheating mode

On this mode the coolant is circulated by the pump with PTC heating and the battery group begins to generate heat when its temperature gets to be higher than 0°C .

Fig.8 shows the temperature response of the battery preheating process under -20°C out-car temperature. The coolant average temperature increases quickly as the PTC heater is on. But the battery response temperature does not change at the first stage of 200s until the coolant temperature goes up to be 2°C . After then it begins to increase

gradually with the increasing of the coolant temperature. This means the heat pipe also has a start condition on heating mode. The start temperature of its bottom evaporating terminal is about 2°C and the temperature difference between the evaporating terminal and condensing terminal under this condition is about 22°C. The battery begins to generate heat as its temperature gets higher than 0°C, so the increase rate of the battery temperature is getting higher after 0°C.

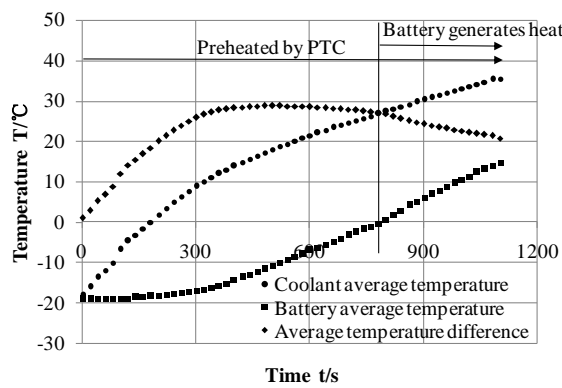


Fig.8 Temperature response on preheating mode

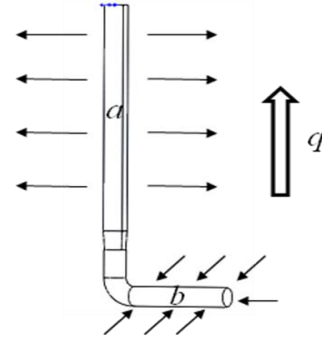


Fig.9 Heat transfer way of the heat pipe

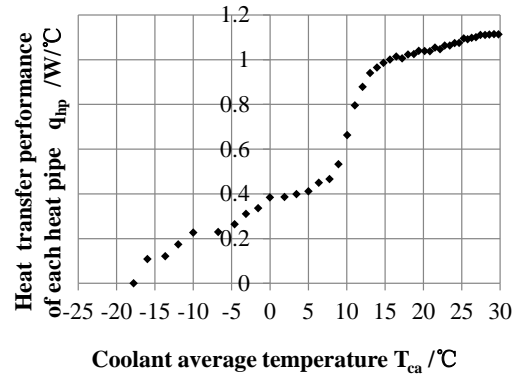
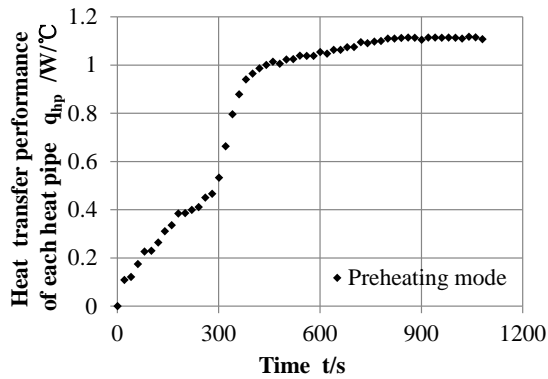


Fig.10 Heat transfer performance on preheating mode

Fig 9 shows the heat transfer way of the heat pipe under preheating mode. The bottom part *b* of the heat pipe absorbs heat from coolant and the top part *a* preheats the battery. The fluid inside of the heat pipe evaporates at the bottom part, goes up to the top part by the central route of the pipe with the heat and gets down by the inside

wall of the pipe after condensation. Fig.10 shows the heat transfer performance of each heat pipe on preheating mode. At first the heat transfer performance increases gradually at a relative low level with the increasing of the temperature difference. As the coolant temperature goes up to be higher than 8°C, the heat transfer performance jumps up quickly to a higher value, and then increases slowly to a relative stable value, which is about 1.11W/°C. This result verifies that the coolant temperature has important effect on the heat transfer performance of the HPHE because the evaporating and condensing process of the fluid inside of the heat pipe depends on the temperatures of its two terminals. Meanwhile, compare to the heat transfer performance of the heat pipe on cooling mode, that on heating mode is higher. This is because on heating mode the heat pipes can take advantage of the gravity role to get better heat transfer performance. The HPHE designed for this experimental bench can be on a good heat transfer performance when the coolant average temperature is higher than 15°C.

4. Conclusion

According to the above experimental research on an integrated thermal management system for EV, the cooling and heating performance of heat pump system and heat transfer performance of HPHE are investigated. The research results show that the presented system works well as an effective thermal management method for EV. The main conclusions go as following:

320 (1) The system cooling performance shows that the additional parallel branch of
321 battery chiller is a good way to solve the battery group cooling problem, which can
322 supply about 20% additional cooling capacity without input power increase. The
323 cooling capacity distribution of each branch under different working conditions can
324 be optimized by adjusting the expansion valve.

325 (2) The system heating performance under extremely cold condition shows that
326 although the heating COP under -20°C in-car temperature is higher than that under
327 20°C , the compression efficiency of the scroll compressor is much lower because the
328 motor efficiency of scroll compressor drops rapidly under lower load conditions. So
329 improving the heating performance under high temperature difference condition is
330 still an important future work for EV.

331 (3) The specific heat of the battery group is tested about $1.24\text{ kJ/kg}^{\circ}\text{C}$. On cooling
332 mode, there is a delay for the HPHE to start heat transfer and the temperature
333 difference for the HPHE to start between its two terminals is about $7\sim 8^{\circ}\text{C}$. The heat
334 pipe heat transfer performance on different cooling working conditions is around 0.87
335 $\text{W}/^{\circ}\text{C}$.

336 (4) On preheating mode, the HPHE also has a necessary start condition. The start
337 temperature of the bottom evaporating terminal is about 2°C and the temperature
338 difference between the two terminals is about 22°C . The coolant temperature has
339 important effect on the heat transfer performance of HPHE. As the coolant
340 temperature goes up to be higher than 8°C , the heat transfer performance jumps up

quickly to a higher value, and then increases slowly to a relative stable value, which is about 1.11W/°C. The heat transfer performance of the heat pipe on preheating mode, is higher than that on heating mode because it can take advantage of the gravity role.

(5) The research results show that the heat transfer performance of HPHE can meet the demand of battery temperature control on different working conditions. According to the heat transfer performance of the HPHE and specific heat of the battery group, the design parameters of the coolant system can be determined based on the calculation methodology in the real applications.

5. Acknowledgements

We would like to thank the support by the Natural Science Foundation of China (No. 51576203) and the External Cooperation Program of BIC, Chinese Academy of Sciences (No. 1A1111KYSB20130032)

6. References

- [1] Chen Y, Evans JW. Heat transfer phenomena in lithium/ polymer- electrolyte batteries for electric vehicle application. Journal of the Electrochemical Society. 1993; 140:6.
- [2] Song L, Evans JW. The thermal stability of lithium polymer batteries. Journal of Electrochemical Society.1998; 145: 2327-2334.
- [3] Sato N. Thermal behavior analysis of lithium-ion batteries for electric and hybrid vehicles. Journal of Power Sources, 2001; 99:70-77.

-
- 361 [4] Khateeb SA, Amiruddin S, et al. Thermal management of Li-ion battery with
362 phase change material for electric scooter: experiment validation. *Journal of Power*
363 *Sources*, 2005; 142:345-353.
- 364 [5] Pesaran AA. Battery thermal models for hybrid vehicle simulations. *Journal of*
365 *Power Sources*. 2002; 110: 377-382.
- 366 [6] BEHR. Thermal Management for Hybrid Vehicles. Technical Press Day. 2009.
- 367 [7] Mahamud R, Park C. Reciprocating air flow for Li-ion battery thermal
368 management to improve temperature uniformity. *Journal of Power Sources*. 2011;
369 196(13):5685–96.
- 370 [8] Wu MS, Liu KH, Wang YY, Wan CC. Heat dissipation design for lithium-ion
371 batteries. *Journal of Power Sources* 2002;109(1):160
- 372 [9] Al Hallaj S, Selman JR. A novel thermal management system for electric vehicle
373 batteries using phase-change material. *Journal of Electrochemical Society*. 2000;
374 147(9):3231.
- 375 [10] Ling Z, Chen J, et al. Experimental and numerical investigation of the application
376 of phase change materials in a simulative power batteries thermal management system.
377 *Applied Energy*. 2014;121:104-113.
- 378 [11] Wang T, Tseng KJ, et al. Thermal investigation of lithium-ion battery module
379 with different cell arrangement structures and forced air-cooling strategies. *Applied*
380 *Energy*. 2014;134:229-238.
- 381 [12] Zhao JT, Rao ZH, Li YM. Thermal performance of mini-channel liquid cooled

382 cylinder based battery thermal management for cylindrical lithium-ion power battery.
383 Energy Conversion and Management.2015;103: 157–165

384 [13] Khateeb SA, Amiruddin S. et al. Thermal management of Li-ion battery with
385 phase change material for electric scooter: experiment validation. Journal of Power
386 Sources, 2005;142:345-353.

387 [14] Kim US, Shin CB, Kim CS. Modeling for the scale-up of a lithium-ion polymer
388 battery. Journal of Power Sources. 2009; 189:841-846.

389 [15] Yang X, Yan YY, Mullen D. Recent developments of lightweight, high
390 performance heat pipes. Applied Thermal Engineering. 2012; 33-34:1-14.

391 [16] Esen M, Esen H. Experimental investigation of a two-phase closed
392 thermosyphon solar water heater. Solar Energy. 2005; 79(5):459-468.

393 [17] Remeli MF, Date A, Ding LC, et al. Experimental investigation of combined heat
394 recovery and power generation using a heat pipe assisted thermoelectric generator
395 system. Energy Conversion and Management. 2016; 111: 147-157.

396 [18] Rao Z, W SH. Experimental investigation on thermal management of electric
397 vehicle batterywith heat pipe. Energy Conversion and Management. 2013; 65:92-97.

398 [19] Wang Q, Zou HM, Yan. YY, et al. Experimental investigation on EV battery
399 cooling and heating by heat pipes. Applied Thermal Engineering. 2015, 88:54-60.

400 [20] Suzuki T, Ishii K. Air conditioning system for electric vehicle. SAE technical
401 paper no. 960688.

402 [21] Hosoz M, Direk M. Performance evaluation of an integrated automotive air
403 conditioning and heat pump system. Energy Conversion and Management. 2006; 47:

404 545-559.

405 [22] Direk M, Hosoz M, et al. Experimental performance of an R134a automobile
406 heat pump system coupled to the passenger compartment. World renewable energy
407 congress 2011. Sweden.

408 [23] Qi ZG. Advances on air conditioning and heat pump system in electric vehicles –
409 A review. Renewable and Sustainable Energy Reviews. 2014;38: 754-764.

410 [24] Qin F, Zou HM, Tian CQ, et al. Experimental investigation on heating
411 performance of heat pump for electric vehicles at -20 °C ambient temperature. Energy
412 Conversion and Management.2015;102: 39-49.

413 [25] Qin F, Zou HM, Tian CQ, et al. Experimental investigation and theoretical
414 analysis of heat pump systems with two different injection portholes compressors for
415 electric vehicles. Applied Energy. 2016, In Press.